Chimica Techno Acta
published by Ural Federal University
eISSN 2411-1414
chimicatechnoacta.ru

ARTICLE
2023, vol. 10(2), No. 202310207
DOI: 10.15826/chimtech.2023.10.2.07

Crystallization kinetics of GdYScAlCo high-entropy bulk metallic glass

V.A. Bykov [a], D.A. Kovalenko [b *], E.V. Sterkhov [a], T.V. Kulikova [a]

a: Institute of Metallurgy, Ural Division of Russian Academy of Sciences, Ekaterinburg 620002, Russia
b: Ural Federal University, Ekaterinburg 620009, Russia
* Corresponding author: darya.k.2000@list.ru

This paper belongs to a Regular Issue.

Abstract

The thermal stability and non-isothermal crystallization of a new bulk-amorphous high-entropy (HE-BMG) equiatomic GdYScAlCo alloy were studied by differential scanning calorimetry (DSC). The alloy shows a four-stage crystallization process. The kinetic parameters (activation energy (E_α)), the pre-exponential factor (log$A$) and glass-forming ability indicators (kinetic fragility index, characteristic temperatures) for the GdYScAlCo alloy were obtained. The E_α values obtained by isoconversional methods indicate a nonlinear Arrhenian behaviour and a complex process. The Avrami equation modification proposed by Jeziorny and the multivariate nonlinear regression method were applied on the nonisothermal crystallization. In the case of primary crystallization of the amorphous GdYScAlCo alloy under nonisothermal conditions, the kinetics of the nucleation process is best described by an autocatalytic reaction.

Keywords

high-entropy bulk metallic glass
activation energy
glass-forming ability
primary crystallization

Received: 13.03.23
Revised: 04.04.23
Accepted: 11.04.23
Available online: 18.04.23

Key findings

- New bulk-amorphous high-entropy equiatomic GdYScAlCo alloy was produced.
- Non-isothermal crystallization kinetics of GdYScAlCo metallic glass was investigated.
- The multivariate nonlinear regression method suggested a combined auto-catalysis reaction model.

1. Introduction

Since the first discovery in 1960, interest in metal glasses and other metastable materials has been growing [1]. For more than 60 years of research, several hundred bulk metallic glasses (BMG) were synthesized with dimensions up to tens of centimeters. The majority of the synthesized BMGs are alloys based on one or two basic elements with small additions of elements that increase glass-forming ability and characteristics of materials [2–4]. In addition to high glass-forming ability, such materials have a number of unique properties: high thermal stability, high plasticity and soft magnetic properties.

Also, amorphous alloys based on Sc–Al–Co have unique strength and corrosion characteristics [5]. Additionally, additives of rare-earth metals (REM) affect the glass-forming ability (GFA) of these alloys. For example, REM additives (Gd, Y) increase the glass-forming ability and improve the mechanical properties of Sc–Al–Co alloys [5].

However, the GFA and thermal stability of GdYScAlCo alloys, as well as the mechanisms of their crystallization, is not studied. We chose an equiatomic GdYScAlCo alloy for research because it easily amorphizes under arc melting conditions. To estimate the GFA, we used various experimental indicators of glasses, such as glass transition temperature (T_g), on-set crystalline temperature (T_x) and liquidus temperature (T_l), etc.

To obtain given properties of the GdYScAlCo alloy, as well as to predict the optimal compositions and heat treatment modes, the calculation of kinetic parameters (activation energy E_a, pre-exponential factor) using iso-conversion methods of thermal analysis was carried out.

2. Experimental procedure

2.1. Materials and synthesis

The master equiatomic GdYScAlCo alloy was prepared by arc melting Al (99.99% purity), Gd (99.9%), Y (99.9%), Sc (99.9%) and Co (99.9%) in a helium atmosphere. Further, it is re-melted five times to achieve complete melting and compositional homogeneity. The composition of the samples was controlled by weighing them before and after synthesis, and the mass loss did not exceed 0.1 wt.%. Then, amorphous alloy was produced by performing suction casting of the arc-melted metal liquid into a copper mold to produce a 3 mm diameter rod.

2.2. Differential scanning calorimetry (DSC) and X-ray diffraction measurements

The as-cast rod structure was examined by X-ray diffraction at room temperature in a 2θ angular range of 25°–100° at a step of 0.004° using a Shimadzu XRD7000 diffractometer and Cu Kα radiation; the exposition time was 3 s. Thermal reactions in the sample were investigated by differential scanning calorimetry using a Netzsch STA 449C device, calibrated with indium, tin zinc, aluminum, silver and gold standards. The selected sample mass was $20.1\pm0.1\cdot10^{-6}$ kg. DSC scans were performed at different heating rates (5, 10, 20, 40 K/min) in the temperature range from 273 to 1100 K at an argon flow of 60 ml/min. To describe the initial crystallization process and to determine the kinetic parameters, NETZSCH Kinetics Neo software (NETZSCH, Selb, Germany) was applied using model-free and the multivariate nonlinear regression methods.

3. Results and Discussion

3.1. Thermal analysis and GFA indicators

Figure 1 illustrates an X-ray pattern of the GdYScAlCo rod that shows an amorphous halo without distinct crystalline peaks, i.e., the resulting sample is X-ray amorphous.

The non-isothermal DSC of of GdYScAlCo HE-BMG are shown in Figure 2. All the DSC curves exhibit the four exothermic reactions corresponding to the crystallization processes. Table 1 shows the thermal characteristics of the GdYScAlCo alloy: glass transition temperature T_g, on-set crystalline temperature T_x, melting temperature T_m, liquidus temperature T_l, as well as indicators of glass-forming ability: supercooled liquid interval $\Delta T_x = T_g - T_x$, $T_{rg} = T_l/T_g$ and melting interval $\Delta T_l = T_l - T_m$. GdYScAlCo alloy shows high values of glass transition temperature T_g.

GFA is related to physical nature of alloy and reflects how well the alloy forms metallic glass during casting. There are various criteria for evaluating GFA, including γ and δ, which are based on the classical theory of nucleation [6]. These criteria can be easily obtained by thermal analysis and show a strong correlation with GFA in metallic glasses. Calculation of γ and δ criteria was carried out according to equations:

$$\delta = \frac{T_x}{(T_l - T_g)}, \quad (1)$$

$$\gamma = \frac{T_x}{(T_l + T_g)}. \quad (2)$$

In paper [7] for the four-component $Sc_{36}Al_{24}Co_{20}Y_{20}$ alloy the value of the criterion γ = 0.444 was presented, which agrees well with our data for the five-component GdYScAlCo alloy (γ = 0.407). Table 1 shows the criteria γ and δ, which indicate a good glass forming ability of the GdYScAlCo alloy.

The term “fragility” introduced by Angel [8], shows the degree of deviation of the temperature dependence of the viscosity from the Arrhenius curve and is a GFA indicator. From the physical perspective, it characterizes how well the material transitions to the glass state when cooled. Substances with high values of this parameter have a narrow range of glass transition temperatures, while substances with low values have a relatively wide range [8].

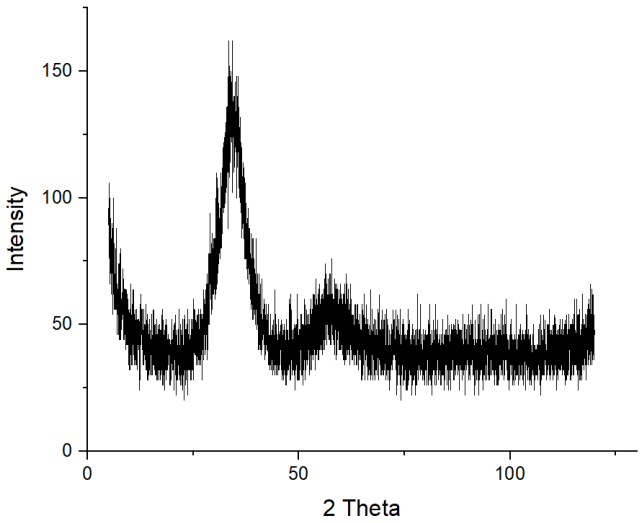

Figure 1 XRD pattern of the GdYScAlCo rod.

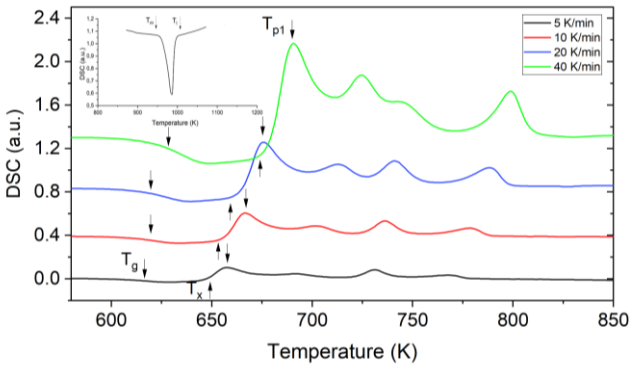

Figure 2 Experimental DSC curves of GdYScAlCo amorphous alloy at different heating rates (inset: temperatures T_m, T_l for heating rate of 10 K/min).

 DOI: 10.15826/chimtech.2023.10.2.07

Table 1 Thermal characteristics for GdYScAlCo alloy according to DSC measurements obtained at a rate of 10 K/min.

Alloy	T_g, K	T_x, K	T_m, K	T_l, K	ΔT_x	T_{rg}	ΔT_l	γ	δ
GdYScAlCo	559	631.5	960	992	32	0.563	32	0.407	1.458

Fragility is determined by the slope of the viscosity curve according to the dependence of log (viscosity) on T_g/T when approaching T_g, which gives the kinetic index of a Fragility (m). The kinetic a Fragility index can be obtained as follows [9]:

$$m = \frac{DT_0T_g}{(T_g - T_o)^2 \ln 10}, \quad (3)$$

where D is the strength parameter, T_0 is the asymptotic value of T_g at an infinitely slow cooling and heating rate, and T_g is the glass transition temperature [8]. D and T_0 can be determined through the relationship between T_g and heating rate (β) by an equation with the Vogel-Fulcher-Tammann form [10]:

$$\ln\beta = \ln(B) - \frac{DT_0}{T_g - T_0}. \quad (4)$$

Fragility index for the sample was calculated at heating rates 5, 10, 20, 40 K/min. The data obtained from Equations 3 and 4 are summarized in Figure 3. The results show that m is equal to 33. The liquids with the fragility index m close to 17 are usually referred to "strong" glass-formers. The liquids with m much higher than 17 are usually referred to "fragile". In the case of GdYScAlCo HE-BMG, it can be classified into "fragile" glasses.

The parameter F_1, introduced by Senkov [11], is an indicator of glass-forming ability, which establishes a correlation between the fragility parameter and the critical cooling rate at which the amorphous state is formed. The value F_1 = 0 corresponds to an extremely fragile liquid, and F_1 ~ 0.8 – extremely strong liquid.

The F_1 parameter can be defined as:

$$F_1 = \frac{(T_g - T_0)}{0.5(T_l + T_g) - T_0}, \quad (5)$$

where T_g is the glass transition temperature, T_l is the liquidus temperature, and T_o is the on-set temperature.

The calculation results are presented in Table 2.

Compared to other metallic glasses: $La_{55}Al_{25}Ni_{20}$ (m = 42, F_1 = 0.455), $La_{55}Al_{25}Ni_{10}Cu_{10}$ (m = 35, F_1 = 0.540) [11], the alloy GdYScAlCo shows rather high values in frazilite and the F_1 parameter, which indicates its good glass forming ability.

3.2. Primary crystallization kinetics of GdYScAlCo

3.2.1. Activation energy

One of the most important kinetic parameters of the crystallization process is the activation energy. It represents the energy barrier that must be overcome by the system to start the nucleation and growth process leading to crystallization.

According to Figure 2, there are four crystallization peaks on the DSC curves. Since the first peak overlaps with the second and third ones, we used a mathematical procedure of peak shape separation to correctly estimate the kinetic parameters of the nucleation and primary crystallization process (Figure 4) [12]. In the calculations we used the DSC peaks at different heating rates obtained by deconvolution, so they should be compared. The separated peaks have the same shape at different heating speeds, i.e., they are identical to each other. As can be seen in Figure 4, the positions of onset and peak maximum temperatures of the original DSC signal and the separated ones are almost the same. The baseline was a straight line. Because the crystallization of amorphous alloy is a multistage process, it requires additional structural studies. Here, we limit ourselves to calculating the kinetic parameters only for the first peak and describing the mechanism of nucleation and primary crystallization. Thus, the DSC curves (Figure 2) show peaks corresponding to the nucleation and crystal growth processes. We calculate the activation energies corresponding to these temperatures to understand the nucleation and crystallization in general.

In the methods of non-isothermal kinetics based on the free model, it is assumed that the single-step processes occurring can be described following rate equation [13]:

$$\beta\frac{da}{dt} = Af(a)e^{\frac{-E_a}{RT}}, \quad (6)$$

where A is the pre-exponential factor, β – the constant heating rate, E_α is the activation energy, and the concentration dependence of the reaction rate (reaction model) is $f(a)$, where a is the degree of transformation of the substance in the range from 0 to 1.

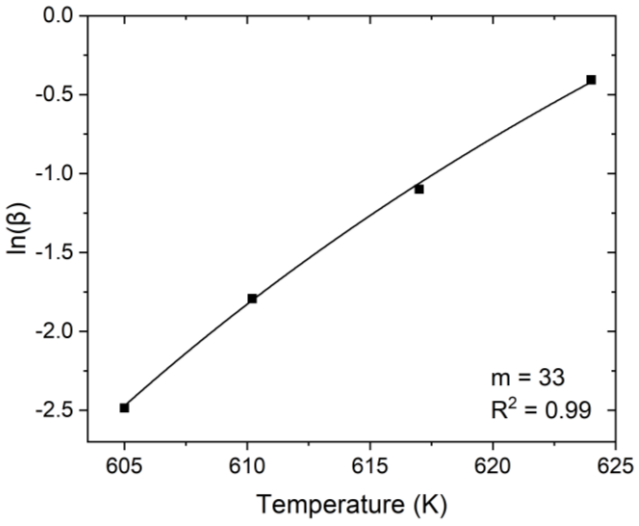

Figure 3 Fragility index for GdYScAlCo alloy.

Table 2 T_g, T_l, m and F_1 parameter for GdYScAlCo alloy.

T_g (K)	T_l (K)	m	F_1
559	992	33	0.463

 DOI: 10.15826/chimtech.2023.10.2.07

Additionally, it was assumed that the reaction rate at a constant conversion value depends only on temperature (iso-conversion principle). It should be noted the importance of determining the preexponential factor A in the framework of kinetic analysis without using a model. According to Vyazovkin [14] model-free method of estimating the preexponential factor A is suitable for both single- and multi-step kinetics. Model-free methods of analysis allow us to determine the activation energy E_α of the reaction process without making hypotheses about the kinetic model of the process and without knowing the type of reaction [13]. Various model-free methods are used to calculate the activation energy E_α of non-isothermal reactions at different heating rates [15–17]. First, we used the most common of them, the Kissinger method. The basic equation of the Kissinger method is written as

$$\ln(\beta/T^2) = -E/RT + \text{const}, \quad (7)$$

where β is the heating rate, R is the gas constant, T is the temperature.

Figure 5 shows the dependences described by equation (2), which correspond to the following processes: the glass transition at $T_g(E_g)$; the start of nucleation at $T_x(E_x)$; the crystal growth at $T_{p1}(E_{p1})$. The calculation results of the activation energy are shown in Figure 5 and Table 3.

Table 4 shows that the highest activation energy is at the beginning of the nucleation process, E_x = 314 kJ/mol. This suggests that the most energy-consuming process is the beginning of crystallization (the appearance of the first nuclei of the crystalline phase in the amorphous matrix).

Thus, we determined the activation energy of the primary crystallization process (E_p) using the Kissinger equation (Equation 7). However, from a physical viewpoint, this method cannot be applied directly to amorphous alloys, since the crystallization process in them proceeds through the nucleation and crystal growth processes rather than through the n-order reaction [18, 19]. Also, as noted by Vyazovkin [13], Kissinger's method is not very accurate. The method gives a single activation energy in accordance with the assumption of one-step kinetics, which creates a problem for most applications.

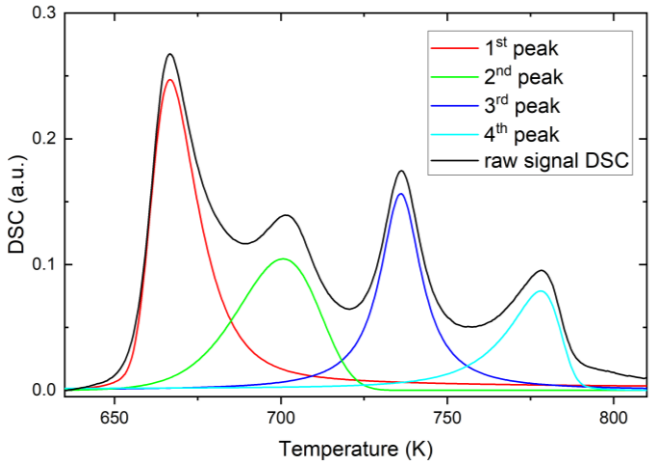

Figure 4 Separated DSC curves for a heating rate of 10 K/min.

We performed calculations of E_α using other model-free methods (Vyazovkin [15], Friedman [16] and Ozawa [17]) in the NETZCH Kinetics Neo software. The calculation results by Kissinger, Vyazovkin, Friedman and Ozawa methods are presented in Table 4 and Figure 5. The analysis of the dependence of E_α versus α (conversion) of the crystallization process of the HE-BMG GdYScAlCo alloy obtained from isoconversional methods (Ozawa, Friedman and Vyazovkin) allows us to check the applicability of the one-step kinetics according to Equation 7.

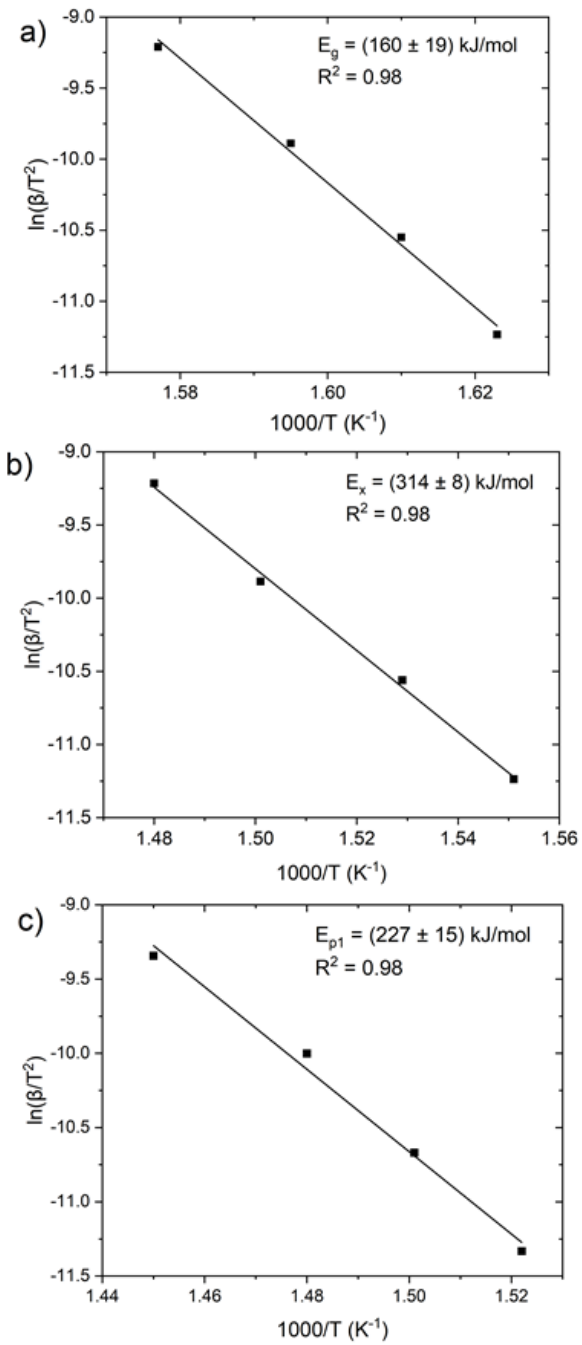

Figure 5 Kissinger plots for calculating activation energies in GdYScAlCo BMG.

Table 3 Activation energy E_g, E_x, E_{p1} for temperatures T_g, T_x, T_{p1}.

Alloy	Activation energy, kJ/mol		
	E_g	E_x	E_{p1}
GdYScAlCo	160	314	227

DOI: 10.15826/chimtech.2023.10.2.07

Figure 4 presents the dependence of the E_α and log$A$ on the degree of conversion calculated using Ozawa, Friedman and Vyazovkin methods. We can see from Figure 6 that the values of $E(\alpha)$ change nonlinearly, where as the dependences of $E(\alpha)$ are similar. The Eα values indicate a nonlinear Arrhenian behaviour and a complex process. The close average $E(\alpha)$ values obtained by the conversional methods differ from those calculated with Kissinger's method. Therefore, the Kissinger method can only be used for preliminary estimation of the activation energy of a one-step process. Due to the fact that the values of $E(\alpha)$ change nonlinearly and indicate a complex process, naturally, the Kissinger activation energy values cannot be applied when simulating the complex process of crystallization of amorphous materials, where multistage processes are observed.

Table 4 Crystal growth activation energy E_{p1} and pre-exponential factor log A for GdYScAlCo alloy.

Kinetic parameter	Vyazovkin	Kissinger method	Friedman	Ozawa-Flynn-Wall	Average value
E_{p1},	250	227	250	260	247
log$A$	17.6	13.1	17.6	17.8	16.5

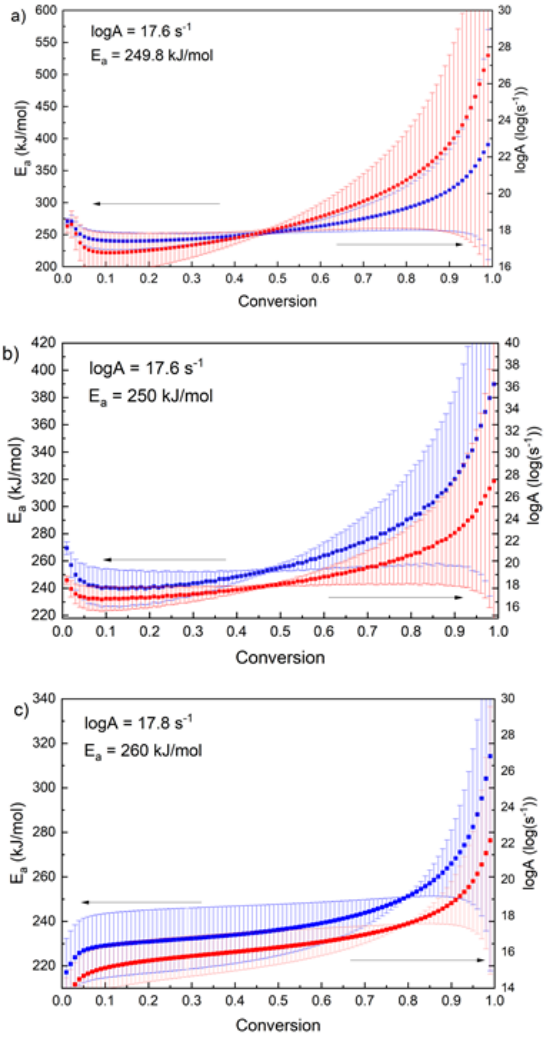

Figure 6 Activation energy and log$A$ values of versus conversion during the crystallization process using the Friedman (a), Vyazovkin (b), and Ozawa (c) methods.

3.2.2. Avrami model using Jeziorny method

One of the most commonly used models for describing the crystallization kinetics of polymers, metals, and glasses is the Avrami model (also known as the Johnson–Mehl–Avrami–Erofeev–Kolmogorov (JMAEK) model [20–25]). To isothermal conditions, the Avrami equation is typically used in the following form:

$$a\,(T) = 1 - e^{-k(T)\cdot t^n}, \tag{8}$$

where a is the degree of conversion, $k(T)$ represents the rate constant, t is time and n is the local Avrami index.

For nonisothermal experimental conditions, Equation (8) is frequently expressed as the following linear equation:

$$\frac{da}{dt} = \frac{k(T)}{\beta}\cdot n\cdot(1-a)\cdot[-\ln(1-a)]\cdot\frac{(n-1)}{n}. \tag{9}$$

The volume fraction of crystals (conversion a) can be determined by the crystallization heat using the following equation [26]:

$$a = \frac{\int_{T_0}^{T}(dH/dT)dT}{\int_{T_0}^{T_{inf}}(dH/dT)dT} = \frac{A_0}{A_{inf}}, \tag{10}$$

where T_o and T_{inf} are the temperatures of the beginning and end of crystallization, respectively. dH corresponds to the enthalpy of crystallization released during an infinitesimal temperature interval dT. A_o and A_{inf} correspond to the region between the initial and specific temperature and the end of crystallization, respectively. Figure 7 shows the relationship between the volume fraction of crystallization and the temperature for primary crystallization. From Figure 7 we see that with an increase in the heating rate, the S-curves shift to the region of higher temperatures.

Many attempts have been made to derive Equation 8 under non-isothermal temperature with constant heating or cooling rates [27]. The main difficulty in modifying the JMAEK model under non-isothermal conditions is that these experiments are much faster than isothermal experiments.

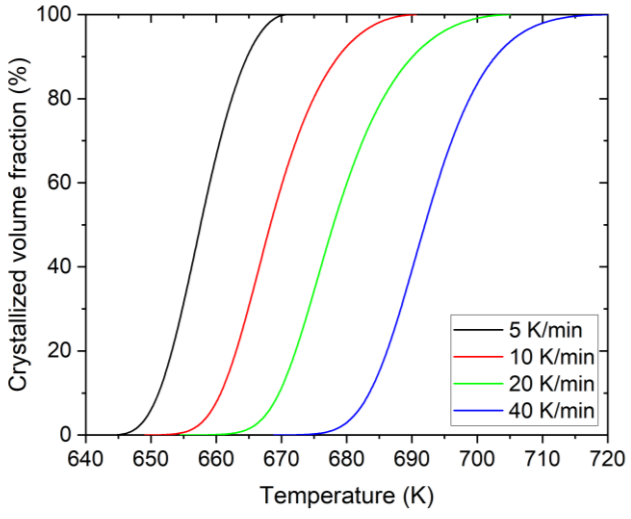

Figure 7 Crystallized volume fraction versus temperature plots.

 DOI: 10.15826/chimtech.2023.10.2.07

In isothermal experiments, the material under study is heated to a certain temperature in a time much shorter than the transformation time. Crystallization of metallic glasses under linear heating conditions is mainly studied using the JMAEK method modified by Jeziorny [28], who converted the linear Avrami equation to linear heating conditions using the following assumption:

$$\ln k_A = \frac{\ln k(T)}{\beta}, \tag{11}$$

where $k(T) = Ae^{\frac{-E_a}{RT}}$ – rate constant, β – heating rate

However, as Vyazovkin states [29], this transformation contradicts the basic principle of equating physical quantities and also leads to incorrect Avrami indices, usually larger than the actual value. It should be noted that the Jeziorny's method is often used to calculate the Avrami index of non-isothermal crystallization kinetics of amorphous metallic glasses due to the developed algorithm for the interpretation of the polymer crystallization mechanism. [30]. However, the crystallization processes in amorphous metallic materials and polymers can be radically different. Further, the mechanism of primary crystallization for the amorphous GdYScAlCo alloy under non-isothermal conditions by the Jeziorny method will be tested in the multivariate nonlinear regression method. To determine the mechanism of nucleation and its growth, we used the approach of determining the local Avrami index $n(\alpha)$ with Jeziorny's assumption (Equation 11), which was proposed in [31]. According to [31], the local Avrami index $n(\alpha)$ can be found from a modification of the JMAEK equation, given that $t-t_o = (T-T_o)/\beta$, where T_o is the temperature at the crystallization onset. Therefore, it can be written as:

$$\frac{d\ln[-\ln(1-\alpha)]}{d\{\ln[(T-T_{0})/\beta]\}} = n\left\{1+\frac{E}{RT}\left(1-\frac{T_0}{T}\right)\right\}, \tag{12}$$

where T_o is the initial crystallization temperature and E is the activation energy of the crystallization process. The values of E in Equation 10 were used as $E(\alpha)$ calculated by the Vyazovkin method.

For non-isothermal DSC curves, the local Avrami index ($n(\alpha)$) can be obtained by plotting the dependence of $\ln[-\ln(1-\alpha)]$ on $\ln[(T-T_o)/\beta]$. The plots of these dependences are shown in Figure 8, where the value of $n(\alpha)$ can be obtained from the slope of these curves. In addition, Figure 9 shows the local Avrami index indices as a function of the volume fraction of crystallized matter α at different heating rates. The resulting curves are not linear, indicating that $n(\alpha)$ changes during the crystallization process. The $n(\alpha)$ is a basic parameter that is necessary to understand the mechanisms of nucleation and grain growth with increasing α during the transformation phase. The local Avrami index is expressed as:

$$n = b + pm, \tag{11}$$

where b is the nucleation index, m is the dimensionality of grain growth and p is the type of growth. The germination index contains four conditions: (1) $b = 0$ suggests a zero germination rate; (2) $0<b<1$ indicates a decrease in the germination rate with time; (3) $b = 1$ represents a constant germination rate; (4) $b>1$ indicates an increase in the germination rate with time. The grain growth magnitude m is 1, 2, or 3; $p = 1$ represents surface-controlled growth, and $p = 0.5$ indicates diffusion-controlled growth.

Before describing the primary crystallisation mechanism using the $n(\alpha)$ dependence, we present an important remark. Since the peak separation procedure performed allows determining the approximate baseline, it must be considered that extreme values of $n(\alpha)$ (both α< and α~1) are unreliable, since they are affected by the baseline.

Figure 8 shows that at the start of the crystallization process, the $n(\alpha)$ values are 2.2–3.5, indicating that the growth mechanism is surface-controlled. The appearance of these curves clearly shows the course of nucleation and grain growth at different heating rates. All $n(\alpha)$ at different heating rates are greater than unity at $x = 0$, which corresponds to the nucleation process with increasing nucleation rate; $n(\alpha)$ of the three curves (10, 20, 40 K/min) firstly increases and then decreases at $0.05 \lesssim x \lesssim 0.91$, which indicates that the nucleation rate and growth dimension always change at this stage. The continuous decrease of $n(\alpha)$ values after a certain percentage of crystallization volume fraction (≳ 5% for speeds 10–40 K/min) shows that nucleation rates decrease to about zero and the grain growth process dominates; all $n(\alpha)$ curves increase rapidly at $0.91 \lesssim x \lesssim 1$.

In the initial stage of crystallization, nucleation dominates, with a constant or increasing rate and no grain growth process when $1 \leq n(\alpha) < 2$; there is one ($n(\alpha) = 2$), two ($2 < n(\alpha) < 3$) or three-dimensional growth ($3 \leq n(\alpha)$) with constant, decreasing or increasing rate of nucleation. In our case, in the initial stage of crystallization the three-dimensional growth of nuclei with increasing nucleation rate is observed.

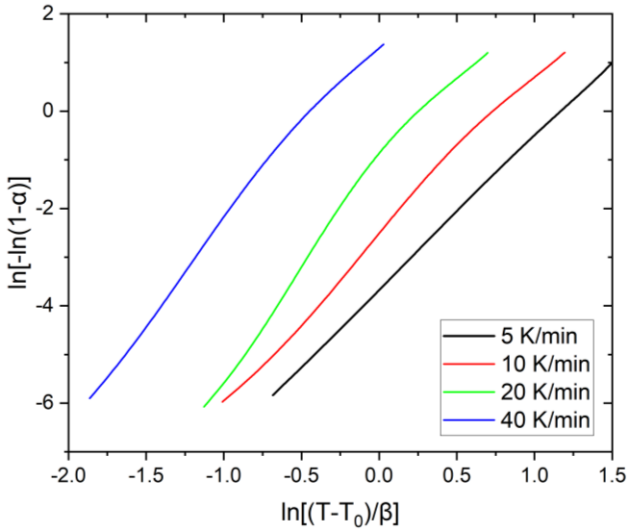

Figure 8 $\ln[-\ln(1-x)]$ versus $\ln[(T-T_{0})/\beta]$ plots at various heating rates (1st DSC peak).

 DOI: 10.15826/chimtech.2023.10.2.07

At 5 K/min, $n(\alpha)$ remains constant until $0.5 \gtrsim x \gtrsim 0.8$, and then increases, indicating that the nucleation process continues at a constant rate. Thus, for the initial stage of crystallization of the amorphous GdYScAlCo alloy, there is a dependence of the nucleation process versus the heating rate.

3.2.3. Avrami model using the multivariate nonlinear regression method

The multivariate nonlinear regression method was also applied to the DSC data of amorphous GdYScAlCo alloy using the Avrami model. This method constructs a kinetic model of the reaction (consecutive, parallel, branched, etc.) and selects the models describing each step. Equations describing kinetic models contain several parameters which are defined by the non-linear regression method from the DSC curves approximation. A comprehensive kinetic analysis using multivariate non-linear regression was performed with NETZSCH Kinetics Neo software [32].

We verified the JMAEK method modified by Jeziorny with respect to all heating curves and the fact that the primary crystallization process is sequential and two-stage (A→B→C). According to the above-described $n(\alpha)$ relationships, the crystallization mechanism of amorphous GdYScAlCo alloy is largely determined by three-dimensional nucleation growth (A→B (A_n)) that is surface-controlled (B→C (R3)). The simulation results and equations of the crystallization models are shown in Figure 10 and Table 5.

Comparative analysis shows satisfactory results (correlation coefficient R^2 = 0.9678); the average values of the Avrami index and E_α are close to those obtained by Equation 12 and Vyazovkin (Friedman, Ozawa).

As calculated, the best correlation coefficient (0.9950) between the separated and simulated DSC curves was obtained by the combined auto-catalysis reaction as two parallel reactive paths (A → B, A+B→2B) according to heterogeneous reaction of n^{th} order with m-Power autocatalysis by-product Kamal-Sourour [33]:

$$\frac{d\alpha}{dt} = Ae^{-\frac{E_{a1}}{RT}} \cdot (1-\alpha)^n + K_{cat} \cdot Ae^{-\frac{E_{a2}}{RT}} \cdot (1-\alpha)^n \cdot a^m, \quad (13)$$

where k_{cat} – auto-catalysis factor, α – conversion, n, m – reaction order, T – temperature.

The results of the simulation and equations of the crystallization model, according to the above proposed primary crystallization scheme of the amorphous GdYScAlCo alloy, are shown in Figure 11 and Table 6.

Thus, based on multivariate nonlinear regression method simulation data, the primary crystallization of the amorphous GdYScAlCo alloy proceeds as a combined auto-catalysis reaction in two parallel reactive paths.

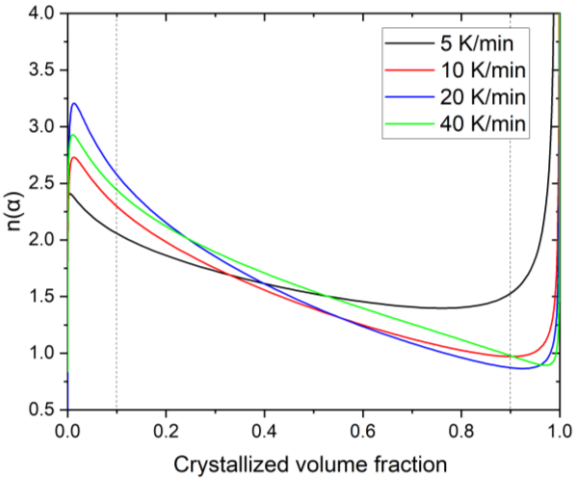

Figure 9 The local Avrami index $n(\alpha)$ versus the volume fraction of crystallization (α).

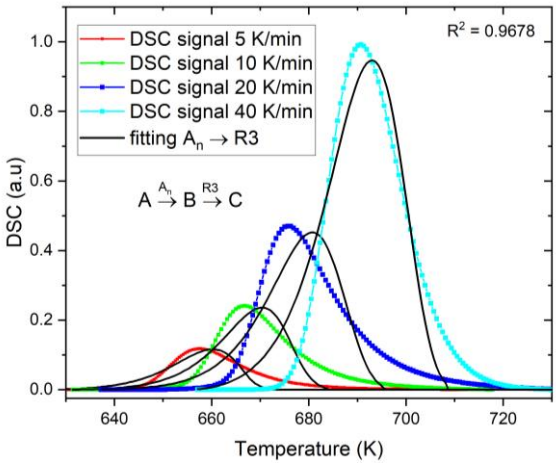

Figure 10 Crystallization model of amorphous GdYScAlCo alloy described by the three-dimensional nucleation growth (A→B (An)) with surface-controlled (B→C (R3)).

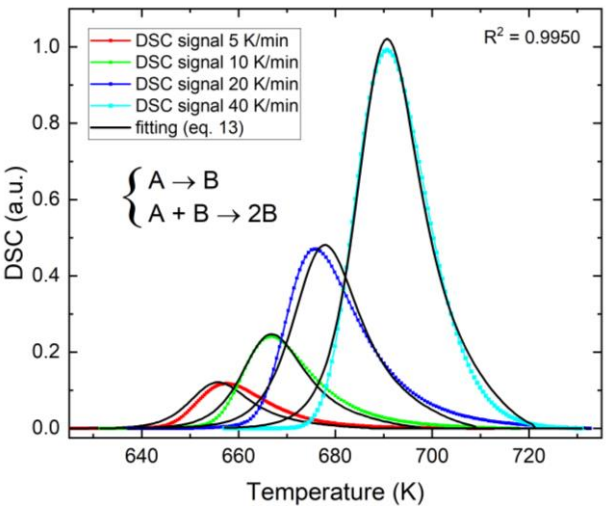

Figure 11 Crystallization model of amorphous GdYScAlCo alloy described by the combined auto-catalysis reaction as two parallel reactive paths (A → B, A+B→2B).

Table 5 Kinetic parameters and the regression coefficient R^2 for the fitting of multivariate nonlinear regression according to two-stage consecutive reactions (three-dimensional nucleation growth (A→B (An)) with surface-controlled (B→C (R3)).

$n_{A->B}$	log$A_{A->B}$, log(s^{-1})	log$A_{B->C}$, log(s^{-1})	$E_{a\ A->B}$, kJ/mol	$E_{a\ B->C}$, kJ/mol	$C_{A->B}$	$C_{B->C}$	R^2
2.1	13.7	25.8	200.1	354.3	0.48	0.52	0.9678

DOI: 10.15826/chimtech.2023.10.2.07

Table 6 Kinetic parameters and the regression coefficient R^2 for the fitting of multivariate nonlinear regression for combined auto-catalysis reaction (heterogeneous reaction with n-th order and m-power autocatalysis).

n	m	log$A$, log(s^{-1})	E_a, kJ/mol	R^2
1.8	0.8	12.7	216.6	0.9950

4. Conclusions

The thermal stability and primary crystallization kinetics of the GdYScAlCo HE-BMG alloy were studied using DSC. The main conclusions are presented below.

1. GdYScAlCo HE-BMG exhibited four different crystallization events. The characteristic temperatures (such as T_{x1}, T_{p1}, T_g...) increased with increasing heating rate. In terms of $m = 33$ and Angel's GdYScAlCo classification, HE-BMG belongs to the "fragile" glasses.

2. The activation energy ($E\alpha$) of the process was calculated using the methods of Vyazovkin, Ozawa, Friedman and Kissinger. The Kissinger method gives inaccurate activation energy values in comparison to the other methods. The $E\alpha$ values obtained by isoconversional methods indicate a nonlinear Arrhenian behaviour and a complex process.

3. Analysis of the crystallization kinetics by Jeziorny's modification of the Avrami model showed that values of the local Avrami index are $1.2<n(\alpha)<3.2$ for approximately the entire initial crystallization period. This means that the crystallization mechanism is largely determined by three-dimensional nucleation growth controlled by the surface as the nucleation rate decreases. As verified by multivariate non-linear regression, the germ growth mechanism in the amorphous GdYScAlCo alloy is satisfactorily described by interface-controlled process.

4. The multivariate nonlinear regression method demonstrated that the primary crystallization of amorphous GdYScAlCo alloy proceeds as a combined auto-catalysis reaction in two parallel reactive paths (A→B, A+B→2B), where the nucleation mechanism is determined by the heterogeneous n-th order reaction (A→B), and grain growth (A+B→2B) by the m-power autocatalysis reaction.

• Supplementary materials

No supplementary materials are available.

• Funding

This work was supported by the Russian Science Foundation (grant no. 23-23-00100), https://www.rscf.ru/en.

• Acknowledgments

None.

• Author contributions

Conceptualization: B.V.A., K.T.V.
Data curation: B.V.A.
Formal Analysis: K.D.A.
Funding acquisition: B.V.A., K.T.V., K.D.A., S.E.V.
Methodology: B.V.A., K.T.V., K.D.A., S.E.V.
Project administration: K.T.V.
Resources: S.E.V.
Software: K.D.A.
Supervision: B.V.A.
Validation: K.D.A., S.E.V.
Visualization: K.D.A.
Writing – original draft: K.D.A., K.T.V.
Writing – review & editing: B.V.A.

• Conflict of interest

The authors declare no conflict of interest.

• Additional information

Authors IDs:
Victor A. Bykov, Scopus ID 55838510460;
Evgeniy V. Sterkhov, Scopus ID 57205360319;
Tatyana V. Kulikova, Scopus ID 7003952401.

Websites:
Institute of Metallurgy, http://www.imet-uran.ru;
Ural Federal University, https://urfu.ru/en.

References

1. Klement W, Willens RH, Duwez Pol. Non-crystalline structure in solidified gold-silicon alloys. Nature. 1960;187:869–870. doi:10.1038/187869b0
2. Yuan R, Yu Z, Leng H, Chou K. Thermodynamic evaluation and experimental verification of the glass forming ability of Cu–Zr-based alloys. J Non Cryst Solids. 2021;564:120835. doi:10.1016/j.jnoncrysol.2021.120835
3. Cui X, Zu FQ, Jiang WX, Wang LF, Wang ZZ. Achieving superior glass forming ability of Zr–Cu–Al–Ni–Ti/Ag bulk metallic glasses by element substitution. J Non Cryst Solids. 2013;375:83–87. doi:10.1016/j.jnoncrysol.2013.05.014
4. Jiang HR, Wei XS, Lu WF, Liang DD, Wen ZH, Xiang HP, Wang Z, Shen J. Design of Cu–Zr–Al and Cu–Zr–Al–Sn bulk amorphous alloys with high glass-forming ability. J Non Cryst Solids. 2019;521:119531. doi:10.1016/j.jnoncrysol.2019.119531
5. Gao K, Zhu XG, Chen L, Li WH, Xu X, Pan BT, Li WR, Zhou WH, Li L, Huang W, Li Y. Recent development in the application of bulk metallic glasses. J Mater Sci Technol. 2022;131:115–121. doi:10.1016/j.jmst.2022.05.028
6. Qingjun Chen, Jun Shen, Deliang Zhang, Hongbo Fan, Jianfei Sun, McCartney DG. A new criterion for evaluating the glass-forming ability of bulk metallic glasses. Mater Sci Engin. 2011;21:164–1172. doi:10.1016/j.msea.2006.06.053
7. Xi XK, Li S, Wang RJ, Zhao DQ, Pan MX, Wang WH. Bulk scandium-based metallic glasses. J Mater Res. 2005;20:2243–2247. doi:10.1557/jmr.2005.0281
8. Angell CA. Formation of glasses from liquids and biopolymers. Sci. 1995;267:1924–1935. doi:10.1126/science.267.5206.1924

 DOI: 10.15826/chimtech.2023.10.2.07

9. Ruocco G, Sciortino F, Zamponi F, De Michele C, Scopigno T. Landscapes and fragilities. J Chem Phys. 2004;120(22):10666. doi:10.1063/1.1736628
10. Brüning R, Samwer K. Glass transition on long time scales Phys Rev B. 1992;46(18):11318-11322. doi:10.1103/PhysRevB.46.11318
11. Senkov ON, Scott JM, Miracle DB. Effect of Al addition of glass forming ability of Ca–Mg–Zn–Cu based bulk metallic glasses. Metall Mater Transact. 2007;39:1901–1907. doi:10.1007/s11661-007-9255-x
12. NETSCH Peak Separation 3. URL: https://analyzing-testing.netzsch.com/ru/blog/2021/separating-overlapping-effects-in-analytical-measurement-curves
13. Vyazovkin S. Kissinger method in kinetics of materials: things to beware and be aware of. Molec. 2020;25:2813. doi:10.3390/molecules25122813
14. Vyazovkin S. Determining Preexponential Factor in Model-Free Kinetic Methods: How and Why? Molec. 2021;26:3077. doi:10.3390/molecules26113077
15. Vyazovkin S. Evaluation of activation energy of thermally stimulated solid-state reactions under arbitrary variation of temperature. J Comput Chem. 1997;18:393–402. doi:10.1002/(SICI)1096-987X(199702)18:3<393::AID-JCC9>3.0.CO;2-P
16. Friedman HL. Kinetics of thermal degradation of char-forming plastics from thermogravimetry. J Polym Sci Part C Polym Symposia. 1964;6(1):183–185.
17. Ozawa Takeo. A new method of analysis thermogravimetric data. bulletin of the chemical society of Japan. Bull Chem Soc Japan. 1965;38:1881–1886. doi:10.1246/bcsj.38.1881
18. Cheng YT, Hung TH, Huang JC, Hsieh PJ, Jang JSC. Thermal stability and crystallization kinetics of Mg–Cu–Y–B quaternary alloys. Mater Sci Engin. 2007;449:501–505. doi:10.2320/matertrans1989.32.609
19. Matusita K, Komatsu T, Yokota R. Kinetics of non-isothermal crystallization process and activation energy for crystal growth in amorphous materials. J Mater Sci. 1984;19(1):291–296. doi:10.1007/bf02403137
20. Avrami M. Kinetics of phase change. I: General theory. J Chem Phys. 1939;7:1103–1112. doi:10.1063/1.1750380
21. Avrami M. Kinetics of phase change. II Transformation-time relations for random distribution of nuclei. J Chem Phys. 1940;8:212–224. doi:10.1063/1.1750631
22. Avrami M. Granulation, phase change, and microstructure kinetics of phase change. J Chem Phys. 1941:177–184. doi:10.1063/1.1750872
23. Shiryayev AN. On the statistical theory of metal crystallization (Ed.), in: A. N. Shiryayev (Ed.), Sel. Work. A. N. Kolmogorov Vol. II Probab. Theory Math Stat. 1992:188–192. doi:10.1007/978-94-011-2260-3_22
24. Barmak K. A commentary on reaction kinetics in processes of nucleation and growth. Mater Sci. 2010;41:2711–2775. doi:10.1007/s11661-010-0421-1
25. Erofe'ev BV. Generalized equation of chemical kinetics and its application in reactions involving solids. Dokl Akad Nauk SSSR. 1946:511–514.
26. Shan Zhang, Chao Wei, Jingwang Lv, Haoran Zhang, Zhilin Sh, Xinyu Zhang, Mingzhen Ma. Non-isothermal crystallization kinetics of the $Zr_{50}Cu_{34}Al_8Ag_8$ amorphous alloy. Mater Lett. 2022;307. doi:10.1016/j.matlet.2021.130996
27. Ruitenberg G, Woldt E, Petford-Long AK. Comparing the Johnson-Mehl-Avrami-Kolmogorov equations for isothermal and linear heating conditions. Thermochim Acta. 2001;378:97–105. doi:10.1016/S0040-6031(01)00584-6
28. Jeziorny A. Parameters characterizing the kinetics of the non-isothermal crystallization of poly(ethylene terephthalate) determined by d.s.c. Polymer (Guildf). 1978;19:1142–1144. doi:10.1016/0032-3861(78)90060-5
29. Vyazovkin S. Jeziorny method should be avoided in avrami analysis of nonisothermal crystallization. Polym. 2023;15:197. doi:10.3390/polym15010197
30. Ozawa T. Kinetics of non-isothermal crystallization. Polymer. 1971;12;3:150–158. doi:10.1016/0032-3861(71)90041-3
31. Blázquez JS, Conde CF, Conde A. Non-isothermal approach to isokinetic crystallization processes: Application to the nanocrystallization of HITPERM alloys. Acta Mater. 2005;53(8):2305–2311. doi:10.1016/j.actamat.2005.01.037
32. Opfermann J. Kinetic analysis using multivariate non-linear regression. I. Basic concepts. J Therm Anal Calorim. 2000;60:641–658. doi:10.1023/A:1010167626551
33. Sourour S, Kamal MR. Differential scanning calorimetry of epoxy cure: isothermal cure kinetics. Thermochim Acta. 1976;14(1–2):41–59. doi:10.1016/0040-6031(76)80056-1

 DOI: 10.15826/chimtech.2023.10.2.07